FULL PAPER

BJC

British Journal of Cancer (2013) 108, 564–569 | doi: 10.1038/bjc.2012.485

Keywords: lymphatic endothelium; ICAM-1; adhesion; CCID; tumour spheroid intravasation

Bay11-7082 inhibits the disintegration of the lymphendothelial barrier triggered by MCF-7 breast cancer spheroids; the role of ICAM-1 and adhesion

K Viola[1,2], S Kopf[1,2], N Huttary[1], C Vonach[1,2], N Kretschy[1,2], M Teichmann[1,3], B Giessrigl[1], I Raab[1], S Stary[1], S Krieger[1], T Keller[1], S Bauer[1], B Hantusch[1], T Szekeres[4], R de Martin[5], W Jäger[6], W Mikulits[2], H Dolznig[3], G Krupitza[1] and M Grusch*[,2]

[1]Institute of Clinical Pathology, Medical University of Vienna, Vienna, Austria; [2]Department of Medicine I, Institute of Cancer Research and Comprehensive Cancer Center, Medical University of Vienna, Borschkegasse 8a, Vienna A-1090, Austria; [3]Institute of Medical Genetics, Medical University of Vienna, Vienna, Austria; [4]Department of Medical and Chemical Laboratory Diagnostics, General Hospital of Vienna, Medical University of Vienna, Vienna, Austria; [5]Department of Vascular Biology and Thrombosis Research, Medical University of Vienna, Vienna, Austria and [6]Department of Clinical Pharmacy and Diagnostics, University of Vienna, Vienna, Austria

Background: Many cancers spread through lymphatic routes, and mechanistic insights of tumour intravasation into the lymphatic vasculature and targets for intervention are limited. The major emphasis of research focuses currently on the molecular biology of tumour cells, while still little is known regarding the contribution of lymphatics.

Methods: Breast cancer cell spheroids attached to lymphendothelial cell (LEC) monolayers were used to investigate the process of intravasation by measuring the areas of 'circular chemorepellent-induced defects' (CCID), which can be considered as entry gates for bulky tumour intravasation. Aspects of tumour cell intravasation were furthermore studied by adhesion assay, and siRNA-mediated knockdown of intracellular adhesion molecule-1 (ICAM-1). Replacing cancer spheroids with the CCID-triggering compound 12(S)-hydroxyeicosatetraenoic acid (HETE) facilitated western blot analyses of Bay11-7082- and baicalein-treated LECs.

Results: Binding of LECs to MCF-7 spheroids, which is a prerequisite for CCID formation, was mediated by ICAM-1 expression, and this depended on NF-κB and correlated with the expression of the prometastatic factor S100A4. Simultaneous inhibition of NF-κB with Bay11-7082 and of arachidonate lipoxygenase (ALOX)-15 with baicalein prevented CCID formation additively.

Conclusion: Two mechanisms contribute to CCID formation: ALOX15 via the generation of 12(S)-HETE by MCF-7 cells, which induces directional migration of LECs, and ICAM-1 in LECs under control of NF-κB, which facilitates adhesion of MCF-7 cells to LECs.

Mostly, metastatic outgrowth demands an early step of intravasation of primary tumour cells into the blood- and lymphatic vasculature, whereby breast cancer cells seem to more commonly frequent the lymphatic route. Therefore, the number of axillary lymph nodes that are colonised by tumour cells is a reliable clinical predictor for patient outcome (Carlson *et al*, 2009). We found that post-sentinel lymph node colonisation and organ invasion correlate with intravasation of tumour cell clusters into lymphatics

*Correspondence: Dr M Grusch; E-mail: michael.grusch@meduniwien.ac.at

Revised 28 August 2012; accepted 4 October 2012; published online 23 October 2012

of sentinel lymph node metastases ('intrametastatic lymphatic carcinosis'; Kerjaschki *et al*, 2011). If intrametastatic lymphatic carcinosis of the sentinel lymph node does not take place, post-sentinel lymph nodes remain metastasis free. Therefore, this step is considered as a critical step for breast cancer cell spread. Lymph node intravasation involves partly the expression of the lipoxygenases arachidonate lipoxygenase (ALOX)-12 and -15, and their metabolite 12(S)-hydroxyeicosatetraenoic acid (HETE), which is secreted, for example, by MCF-7 cells (Uchide *et al*, 2007). *In vitro* 12(S)-HETE causes the retraction of lymphendothelial cells (LECs), thereby causing 'circular chemorepellent-induced defects' (CCID) in LEC walls. CCIDs are the entry gates through which breast cancer cells intravasate (transmigrate) into the lymphatic vasculature. Immunodeficient mice orthotopically xenografted with ALOX15-proficient or -deficient breast cancer cells provided *in vivo* pathophysiological evidence of this mechanism. The relevant protagonists, ALOX12, ALOX15 and 12(S)-HETE, were also detected in paraffin sections of human metastatic lymph nodes, and the expression of ALOX15 correlated inversely with metastasis-free survival of the patients (Kerjaschki *et al*, 2011). The process of intravasation through lymphatics is only partly triggered by 12(S)-HETE, and effectors that act in parallel and/or downstream are unkown. Therefore, the elucidation of the mechanistic details, which are causal for CCID formation, is important. The transcription factor NF-κB has a role in murine lung alveolar carcinoma metastasis, pulmonary metastasis of murine osteosarcomas and lung metastasis of invasive breast cancer MDA-MB-468 cells, orthotopically xenografted in BALB/c nude mice (Andela *et al*, 2000; Srivastava *et al*, 2010; Nishimura *et al*, 2011). Recently it was demonstrated that VE-cadherin expression increased upon inhibition of NF-κB, which stabilised the integrity of LEC monolayers (Vonach *et al*, 2011). Therefore, besides ALOX12/15, NF-κB activity also was involved in compromising lymphendothelial barrier integrity and in CCID formation. In the present work, the interactive process of breast cancer cell intravasation into the lymphatic vasculature was mimicked using a 3D co-culture system, consisting of MCF-7 cancer cell spheroids (Madlener *et al*, 2010) and telomerase-immortalised human LEC monolayers (Schoppmann *et al*, 2004). In particular, the role of NF-κB in the attachment of MCF-7 breast cancer cells to LECs was investigated, which is a prerequisite for tumour cell intravasation.

MATERIALS AND METHODS

Chemicals. The I-κBα phosphorylation inhibitor (E)-3-(4-methylphenylsulfonyl)-2-propenenitrile (Bay11-7082) and baicalein (EI-106) were purchased from Biomol (Hamburg, Germany), 12(S)-HETE from Cayman Chemical (Ann Arbour, MI, USA). Mouse monoclonal anti-CD54 (intracellular adhesion molecule-1, ICAM-1) antibody was from Immunotech (Marseille, France). Monoclonal mouse anti-phospho-p44/42 MAPK (Erk1/2) (Thr202/Tyr204) (E10), monoclonal rabbit anti-p44/42 MAPK (Erk1/2) (137F5), monoclonal rabbit anti-β-tubulin (2128), polyclonal rabbit anti-phospho-myosin light chain 2 (MLC2; Ser19), polyclonal rabbit anti-MLC2 and polyclonal rabbit anti-myosin phosphatase-targeting subunit 1 (MYPT1) were from Cell Signalling (Danvers, MA, USA). Monoclonal mouse anti-β-actin (clone AC-15) and polyclonal rabbit anti-S100A4 were from Sigma-Aldrich (Munich, Germany), polyclonal rabbit anti-phospho-MYPT1 (Thr696) from Upstate (Lake Placid, NY, USA). Monoclonal mouse anti-CD31 (JC70A) as well as anti-mouse and anti-rabbit IgGs were from Dako (Glostrup, Denmark).

Cell culture. Human MCF-7 breast cancer cells were purchased from the American Type Culture Collection (Rockville, MD, USA), and grown in MEM medium supplemented with 10% fetal calf serum, 1% penicillin/streptomycin, 1% non-essential amino acids (Invitrogen; Karlsruhe, Germany). Telomerase immortalised human LECs were grown in EGM2 MV (Clonetics CC-4147; Allendale, NJ, USA), all at 37 °C in a humidified atmosphere containing 5% CO_2. For CCID formation assays, LECs were stained with cytotracker green purchased from Invitrogen.

3D co-cultivation of breast cancer spheroids with LEC monolayers. MCF-7 cells were transferred to 30 ml MEM medium containing 6 ml of 1.6% methylcellulose solution (0.3% final concentration; cat. no.: M-512, 4000 centipoises; Sigma-Aldrich). 150 μl of this cell suspension were transferred to each well of a 96-well plate (Cellstar 650185, Greiner Bio-One; Kremsmünster, Austria) to allow spheroid formation within 48 h. Then, MCF-7 spheroids were washed in PBS and transferred to cytotracker-stained LEC monolayers that were seeded into 24-well plates (Costar 3524, Sigma-Aldrich) in 2 ml EGM2 MV medium.

CCID assay. MCF-7 cell spheroids (3000 cells per spheroid) were transferred to 24-well plates containing LEC monolayers. After 4 h of incubation, the CCID areas in the LEC monolayers underneath the MCF-7 spheroids were photographed using an Axiovert (Zeiss, Jena, Germany) fluorescence microscope to visualise cytotracker (green)-stained LECs underneath the spheroids. CCID areas were calculated with the Axiovision Re. 4.5 software (Zeiss, Jena, Germany). MCF-7 spheroids were treated with solvent (DMSO) as a negative control. Each experiment was performed in triplicate and for each condition, the CCID size of 12 or more spheroids (unless otherwise specified) was measured.

Western blotting. LECs were seeded in 6 cm dishes and treated with the indicated compounds (10 μM Bay11-7082 and or 1 μM 12(S)-HETE). Cells were washed twice with ice cold PBS and lysed in buffer containing 150 mM NaCl, 50 mM Tris pH 8.0, 0.1% Triton-X 100, 1 mM phenylmethylsulfonylfluoride and protease inhibitor cocktail. Afterwards, the lysate was centrifuged at 12 000 r.p.m. for 20 min at 4 °C, and the supernatant stored at −20 °C until further analysis. Equal amounts of protein were separated by SDS polyacrylamide gel electrophoresis and electrotransferred onto Hybond PVDF-membranes (GE Healthcare, Little Chalfont, UK) at 100 V for 1 h at 4 °C. To control equal sample loading, membranes were stained with Ponceau S (Sigma-Aldrich). After washing with PBS/Tween 20 (pH 7.2) or Tris-buffered saline (TBS)/Tween 20 (pH 7.6), membranes were immersed in blocking solution (5% non-fat dry milk in TBS containing 0.1% Tween, or in PBS containing 0.5% Tween 20) at room temperature for 1 h. Membranes were washed and incubated with primary antibodies (in blocking solution; dilution 1 : 500–1 : 1000) by gently rocking at 4 °C overnight or at room temperature for 1 h. Thereafter, the membranes were washed with PBS/Tween or TBE/Tween and incubated with secondary antibodies (peroxidase-conjugated goat anti-rabbit IgG or anti-mouse IgG; dilution 1 : 2000) at room temperature for 1 h. Chemiluminescence was detected by ECL detection kit (Thermo Scientific, Portsmouth, IL, USA), and the membranes were exposed to Amersham Hyperfilms (GE-Healthcare, Buckinghamshire, UK).

Real-Time PCR. LECs were seeded in 12-well plates, then they were pretreated with 10 μM Bay11-7082 for 30 min, and thereafter stimulated with 1.0 μM 12(S)-HETE or with TNF-α (20 ng ml^{-1}). Total RNA was isolated using the RNeasy Mini Kit 50 and QIAshredder 50 (QIAGEN, Hamburg, Germany). An amount of 1.0 μg of total RNA was reverse transcribed with Superscript First Strand Synthesis System (Invitrogen), the resulting cDNA was amplified using TaqMan Universal PCR Master mix (No AmpErase UNG; part no. 4324018; Applied Biosystems, Vienna, Austria) with the E-selectin Primer (TaqMan gene expression assays, part no. 4331182; Applied Biosystems). PCR products were analysed on the Abi Prism 7000 sequence detection system

(Applied Biosystems). Duplicate samples were analysed in parallel. Glyceraldehyde-3-phosphate dehydrogenase served as internal control. Relative transcript expression was calculated using the $\Delta\Delta C_T$ method.

siRNA transfection. One day before transfection, LECs were seeded in a 48-well plate (250 μl per well) and grown in EGM 2 MV medium. On the day of transfection the cells had a confluence of 70%. First, all siRNAs (siRNA ID#: s7086, siRNA ID#: s7087; cat. no.: 4392420) and siRNA negative scramble control (Ambion, Life Technologies, Carlsbad, CA, USA) were re-suspended in nuclease-free water. Then 0.75 μg siRNAs were diluted in culture medium (containing serum and antibiotics) to a final volume of 50 μl. Then, the dilution was mixed briefly by vortexing and 3 μl of a 1 : 4 dilution of RNAiFect Transfection Reagent (Qiagen, cat. no. 301605) were added to the diluted siRNA. Thereafter the dilution was mixed by vortexing for 10 s and incubated for 30 min at room temperature. The cell culture medium was aspirated from the plate and 300 μl of fresh medium (containing serum and antibiotics) were added per well. Then the mix was added drop-wise to the cells and incubated for 8 h at 37 °C. After 8 h the medium was changed and the cells were incubated for 48 h to recover.

Adhesion assay. MCF-7 cells (15 000 per well) were seeded in serum-free medium (DMEM containing 0.5% BSA, 2 mM $CaCl_2$ and 2 mM $MgCl_2$). Then 500 × cytotracker (500 × CytoTracker Solution from CytoSelect tumour-endothelium adhesion assay from Cell Biolabs, Inc., San Diego, CA, USA, cat. no. CBA-215) was added to the cell suspension (2 μl CytoTracker to 1 ml suspension), incubated for 1 h at 37 °C and centrifuged at 1000 r.p.m. for 2 min. Then the medium was aspirated, the cell pellet was washed 3 × with serum-free medium and then re-suspended in EGM2 MV medium. Meanwhile, the medium was aspirated from the endothelial cell culture (in wells of a 48-well plate), collected in Eppendorf tubes, and either Bay11-7082 (15 μM) or DMSO (Sigma-Aldrich) was added. Then, the medium was re-distributed to LEC layers and incubated for 10 min. Also the MCF-7 cell suspension, which was stained with cytotracker, was treated with Bay11-7082 (15 μM) or DMSO and incubated for 10 min at room temperature. Subsequently, the medium was aspirated from the 48-well plate and 200 μl of treated MCF-7 cell suspension were added to each well containing LECs grown in monolayers and incubated for 40 min at 37 °C. Then the medium was aspirated from each well and washed 3 × with 250 μl 1 × wash buffer (10 × wash buffer was from CytoSelect tumour-endothelium adhesion assay). Before the third wash, cells were inspected for morphological changes under the microscope. Then the final wash was aspirated and the plate was tapped on a flint free paper towel. 150 μl of 1 × lysis buffer (4 × lysis buffer was from CytoSelect tumour-endothelium adehsion assay) was added to each well and lysed by the shearing forces through a pipette tip. An amount of

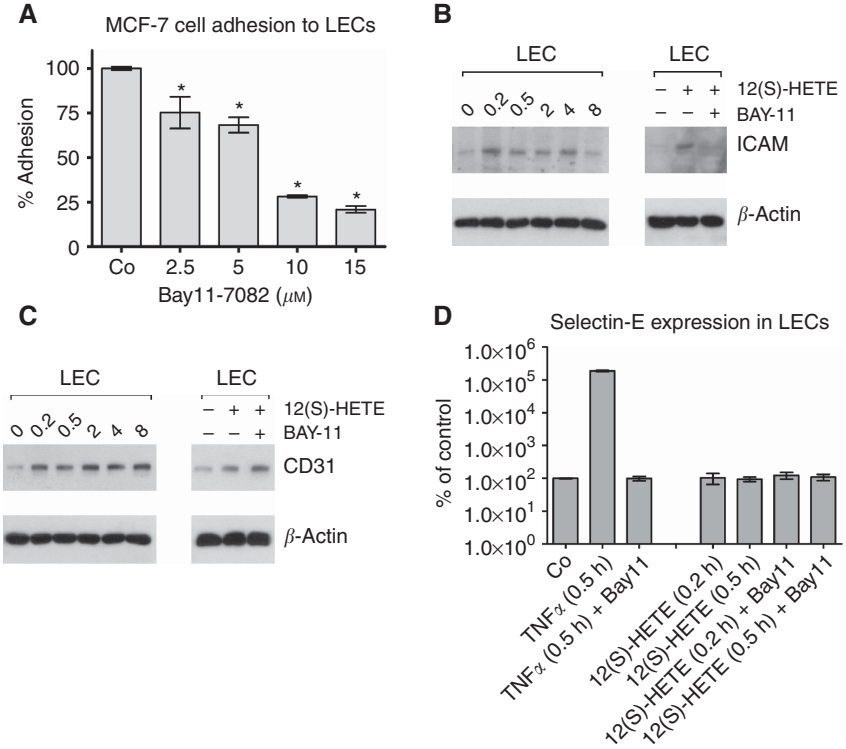

Figure 1. **Inhibition of CCIDs and adhesion protein ICAM-1 by Bay11-7082**. (**A**) Trypsinised and cytotracker-stained MCF-7 cells were placed on LEC monolayers and co-cultivated for 40 min with solvent (DMSO; Co), or with increasing concentrations of Bay11-7082 (2.5, 5, 10 and 15 μM, 0.5 h pretreatment). Then the cells were washed, and the percentages of MCF-7 cells that adhered to LECs were determined by measuring the fluorescence 485/530 nm in the mixed cell lysate. Error bars indicate s.e.m., asterisks significance compared with control ($P<0.05$). (**B** and **C**) LECs growing in six-well plates were treated with 1 μM 12(S)-HETE for 0.2, 0.5, 2, 4 and 8 h (left panels), or LECs were pretreated with 15 μM Bay11-7082 or solvent (DMSO) for 0.5 h, and then stimulated with 1 μM 12(S)-HETE for 0.5 h (right panels). Then, the cells were harvested and protein lysates were analysed by western blotting using antibodies against (**B**) ICAM-1 and (**C**) CD31. Equal sample loading was controlled by β-actin expression. (**D**) Analysis of E-selectin expression. LECs were grown in 12-well plates and pretreated with 15 μM Bay11-7082 for 0.5 h, and thereafter stimulated with 20 ng ml^{-1} TNF-α or solvent (Co) for 0.5 h, or with 1 μM 12(S)-HETE for the indicated times. PCR products were analysed on the Abi Prism 7000 sequence detection system. Duplicate samples were analysed. Glyceraldehyde-3-phosphate dehydrogenase served as an internal control. Relative expression numbers were calculated using the $\Delta\Delta C_T$ method.

100 μl of the lysate were transferred to a 96-well clear bottom plate, and then the fluorescence was read with a fluorescence plate reader at 485/530 nm.

Statistical analysis. Dose-response curves were analysed using Prism 4 software (La Jolla, CA, USA), and significance was determined by Student's *t*-test. Significant differences between experimental groups were $^*P<0.05$.

RESULTS AND DISCUSSION

NF-κB-dependent expression of ICAM-1 contributes to CCID formation. Under physiological conditions, the ALOX12/15 metabolite 12(S)-HETE is mainly produced by platelets, leucocytes, smooth muscle, epithelium, neuron and fibroblast cells (Spector *et al*, 1988) and induces retraction of microvascular endothelial cells (Honn *et al*, 1994; Uchide *et al*, 2007). Under pathophysiological conditions, 12(S)-HETE increases tumour cell adhesion to exposed ECM (Honn *et al*, 1989). 12(S)-HETE is shed by MCF-7 spheroids (Uchide *et al*, 2007) and triggers directional LEC mobility and consequently CCID formation (Madlener *et al*, 2010; Kerjaschki *et al*, 2011; Vonach *et al*, 2011). As the deregulation of NF-κB is associated with cancer development (Folmer *et al*, 2009) promoting oncogenesis through the transcriptional activation of genes associated with cell proliferation, angiogenesis and metastasis (Orlowski and Baldwin, 2002), we focussed on the role of NF-κB in CCID formation. The adhesion of MCF-7 spheroids to LEC monolayers is a prerequisite for CCID formation and increasing concentrations of Bay11-7082 caused the gradual loss of cell adhesion (Figure 1A). Treatment with 25 μM Bay11-7082 completely prevented the attachment of MCF-7 spheroids to LECs and CCID formation (data not shown). Therefore, NF-κB-dependent expression of adhesion molecules could account for the stable contact of MCF-7 spheroids to LECs. CD31, E-selectin (SELE) and ICAM-1 are known to be expressed in endothelial cells. These molecules connect to other cell types through counter-receptors, that is, $\alpha_v\beta_3$ integrin (vitronectin receptor), CD44, and $\alpha_L\beta_2$ integrin (LFA-1), respectively, which were all reported to be expressed in MCF-7 cells (Budinsky *et al*, 1997; Deryugina *et al*, 2000). 12(S)-HETE induced the expression of ICAM-1 and CD31 in LECs, whereas SELE was neither constitutively expressed in LECs nor induced by 12(S)-HETE (Figures 1B–D). As the induction of ICAM-1 (but not the induction of CD31) was inhibited by Bay11-7082, ICAM-1 may have contributed to NF-κB-dependent adhesion of MCF-7 spheroids to LEC monolayers. Specific inhibition of ICAM-1 expression in LECs by siRNAs (Figure 2A) affected the adhesion of MCF-7 cells to LECs, (Figure 2B) and also the formation of CCIDs was attenuated when ICAM-1 expression of LECs was specifically inhibited by siRNA (Figure 2C). Hence, adhesion mediated by ICAM-1 contributes to NF-κB-dependent CCIDs. As CCIDs are the consequence of directional migration of LECs (away from MCF-7 spheroids), mobility proteins were activated (Vonach *et al*, 2011). In 12(S)-HETE-stimulated LECs the treatment with Bay11-7082 inhibited the de-phosphorylation of Erk and the expression of S100A4, which is an angiogenic factor and a marker for a mesenchymal phenotype (Zeisberg and Neilson, 2009) inducing mesenchymal motility and invasiveness of endothelial cells (Takenaga *et al*, 1994; Ambartsumian *et al*, 2001; Jenkinson *et al*, 2004; Schmidt-Hansen *et al*, 2004). Thus, 12(S)-HETE induced a mobile, mesenchymal phenotype in LECs (Vonach *et al*, 2011), which was reversed by Bay11-7082. However, the activating phosphorylation of threonine-696 of MYPT was not prevented by Bay11-7082 (Figure 2D). Therefore, the activity of MYPT was independent of NF-κB and did not correlate with the expression of ICAM-1, indicating that also other mechanisms contributed to LEC plasticity.

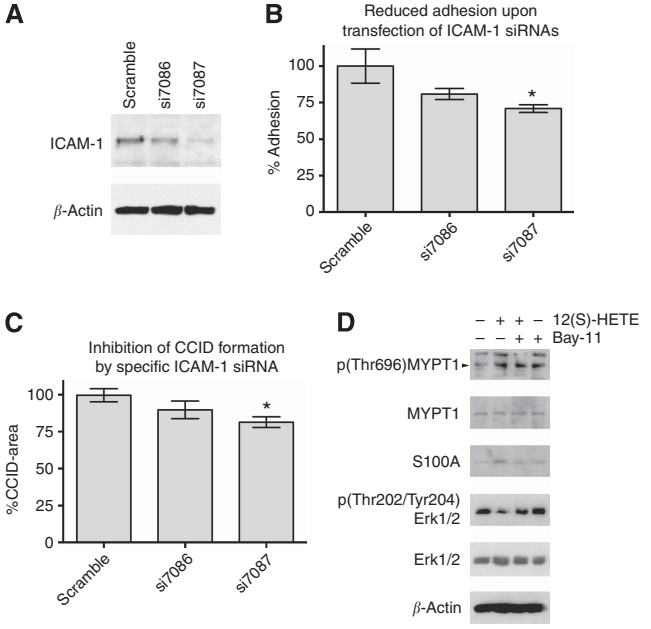

Figure 2. **Inhibition of LEC adhesion and CCID by specific suppression of ICAM-1**. (**A**) LECs growing in six-well plates were transiently transfected with either scramble RNA (control) or siRNAs directed against ICAM-1 (si7086, si7087), and then the expression of ICAM-1 was analysed by western blotting. Equal sample loading was controlled by β-actin expression. (**B**) Trypsinised and cytotracker-stained MCF-7 cells were placed on LEC monolayers that were transiently transfected with siRNAs specifically targeting ICAM-1 (si7086, si7087). Scramble RNA was used as control. After 40 min cells were washed and the percentages of MCF-7 cells that adhered to LECs were determined by measuring the fluorescence 485/530 nm in the mixed cell lysate. (**C**) LECs growing in 24-well plates were transiently transfected with either scramble RNA (control) or siRNAs directed against ICAM-1 (si7086, si7087), and allowed to grow to cunfluence. Then, MCF-7 spheroids were placed on LEC monolayers and co-cultivated for 4 h, and then the areas of CCIDs were measured. Error bars indicate s.e.m., asterisks significance compared with control ($P<0.05$). (**D**) LECs were grown to confluence, and then pretreated with 15 μM Bay11-7082 or solvent (DMSO) for 0.5 h, and then LECs were stimulated with 1 μM 12(S)-HETE for 1 h. Cells were lysed, proteins separated by SDS gel electrophoresis, and subjected to western blotting using the indicated antibodies (migration-related proteins). Staining with Ponceau S and immunoblotting with anti-β-actin antibody controlled equal sample loading.

Simultaneous inhibition of NF-κB- and ALOX activity additively reduces CCID formation. Consistent with the role of ALOX12/15 in the formation of CCIDs was the fact that the ALOX12/15 inhibitor baicalein (100 μM), attenuated LEC-CCID formation by $\sim$50% (Figure 3A). Simultaneous treatment with baicalein plus Bay11-7082 inhibited CCIDs additively. This inhibition was controlled in two ways:

(1) By the CCID-inducing activity of ALOX15, which was restricted to MCF-7 cells because in 12(S)-HETE-stimulated LECs the expression of S100A4, and the phosphorylation patterns of Erk1/2, MYPT1 and MLC2 remained unchanged in presence of baicalein (Figure 3B). It was formerly shown that 12(S)-HETE treatment results in an enhanced phosphorylation of MLC (Rice *et al*, 1998; Vonach *et al*, 2011). Mobility is mediated in microvascular endothelial cells through enhanced phosphorylation (activation) of proteins, comigrating with MLC, actin and vimentin (Tang *et al*, 1993).

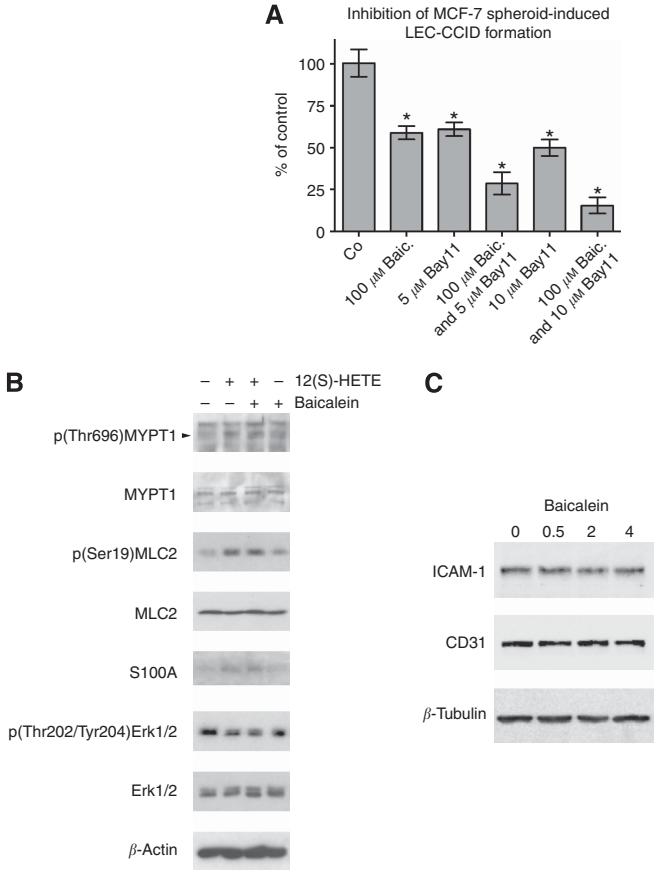

Figure 3. (**A**) Additive inhibition of CCIDs by baicalein and Bay11-7082. MCF-7 spheroids and LEC co-cultures were treated with 10 μM Bay11-7082 and/or 100 μM baicalein for 4 h.Then the CCID areas underneath at least 12 spheroids (per condition) were measured using a Zeiss Axiovert microscope and Axiovision software. Error bars indicate s.e.m., asterisks significance compared with control ($P<0.05$). (**B** and **C**) Analysis of LEC protein expression upon treatment with baicalein. LECs were grown to confluence, and then pretreated with100 μM baicalein or solvent (DMSO) for (**B**) 0.5 h and then LECs were stimulated with 1 μM 12(S)-HETE for 1 h, or (**C**) LECs were treated with 100 μM baicalein for 0.5, 2 and 4 h. Then cells were lysed, proteins separated by SDS gel electrophoresis, and subjected to western blotting using the indicated antibodies. Staining with Ponceau S and immunoblotting with anti-β-actin antibody controlled equal sample loading.

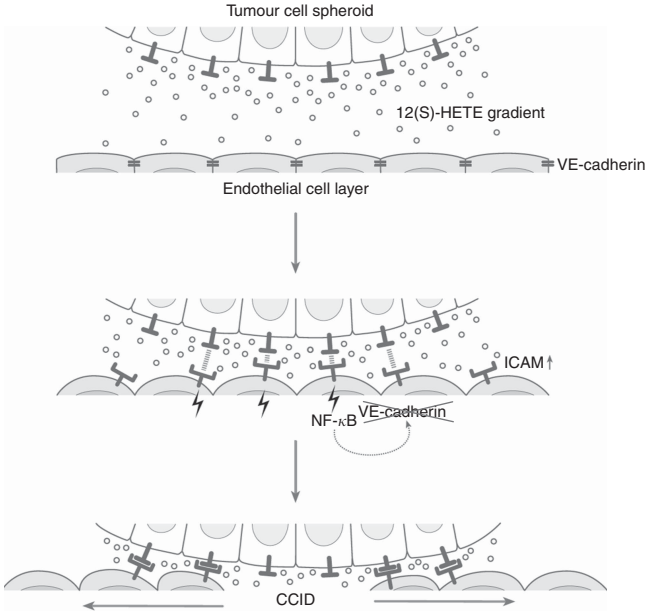

Figure 4. Schematic representation of molecular interactions between MCF-7 spheroids and LEC monolayers. MCF-7 tumour cell spheroids secrete 12(S)-HETE (Uchide *et al*, 2007; Kerjaschki *et al*, 2011), which induces the expression of ICAM-1 in the adjacent LECs by a NF-κB-dependent mechanism. MCF-7 cells adhere to ICAM-1 and tumour spheroids attach to the endothelial monolayers. NF-κB activation downregulates VE-cadherin (Vonach *et al*, 2011), and this facilitates the retraction of LECs triggered by the 12(S)-HETE 'retraction factor' (Honn *et al*, 1994), and finally the formation of CCIDs underneath tumour spheroids. Inhibition of NF-κB inhibits ICAM-1 expression, adhesion to endothelial cells and attenuates formation of CCIDs.

(2) By the CCID-inducing activity of NF-κB, which controlled the expression of ICAM-1 and adhesion of LECs to MCF-7 spheroids (Figures 1A and B). In contrast, baicalein, which is a major inhibitor of CCID formation, did not inhibit the expression of ICAM-1 and CD31 (Figure 3C). The inertia of LECs towards baicalein supported the notion that both CCID-inducing mechanisms were essentially independent of each other (with the exception that 12(S)-HETE induced Bay11-7082-sensitive S100A4 expression).

In conclusion, this study demonstrates that NF-κB controls the adhesion of MCF-7 spheroids to LECs and the formation of CCIDs (Figure 4). The question arises whether alone the adherence of MCF-7 spheroids to LECs (i.e., through ICAM-1) triggers LEC migration or whether additional stimuli are required. It was shown that 12(S)-HETE stimulates NF-κB activation and NF-κB-dependent ICAM-1 expression through RhoA and PKCα (Bolick *et al*, 2005). This indicates that RhoA is an upstream regulator of ICAM-1, and Rho/Rac family GTPases are also prominent regulators of cell migration. Therefore, ICAM-1 expression and LEC motility are most likely parallel, but not serial events. The inhibition of 12(S)-HETE-triggered ICAM-1 expression by Bay11-7082, yet simultaneous persistence of MYPT activation, supported the hypothesis of parallel events.

Co-treatment of the 3D cell system with Bay11-7082 together with the ALOX12/15 inhibitor baicalein exhibited an additive effect on the prevention of CCID formation. These results underscore that several distinct mechanisms contribute to tumour intravasation, and may thus provide targets for interference with the metastatic process.

ACKNOWLEDGEMENTS

We wish to thank Toni Jäger for preparing the figures. A grant of the Fellinger foundation (to GK), grants of the Herzfelder family foundation (to TS, HD and MG), and grants by the Austrian Science Fund, FWF, grant numbers P19598-B13 and P20905-B13 (WM) and by the European Union, FP7 Health Research, project number HEALTH-F4-2008-202047 (WM) are gratefully acknowledged.

REFERENCES

Ambartsumian N, Klingelhofer J, Grigorian M, Christensen C, Kriajevska M, Tulchinsky E, Georgiev G, Berezin V, Bock E, Rygaard J, Cao R, Cao Y, Lukanidin E (2001) The metastasis-associated Mts1 (S100A4) protein could act as an angiogenic factor. *Oncogene* **20**: 4685–4695.

Andela VB, Schwarz EM, Puzas JE, O'Keefe RJ, Rosier RN (2000) Tumor metastasis and the reciprocal regulation of prometastatic and antimetastatic factors by nuclear factor kappaB. *Cancer Res* **60**(23): 6557–6562.

Budinsky AC, Brodowicz T, Wiltschke C, Czerwenka K, Michl I, Krainer M, Zielinski CC (1997) Decreased expression of ICAM-1 and its induction by tumor necrosis factor on breast-cancer cells *in vitro*. *Int J Cancer* **71**(6): 1086–1090.

Bolick DT, Orr AW, Whetzel A, Srinivasan S, Hatley ME, Schwartz MA, Hedrick CC (2005) 12/15-Lipoxygenase regulates intercellular adhesion molecule-1 expression and monocyte adhesion to endothelium through activation of RhoA and nuclear factor-κB. *Artersioscler Thromb Vasc Biol* **25**(2): 2301–2307.

Carlson RW, Allred DC, Anderson BO, Burstein HJ, Carter WB, Edge SB, Erban JK, Farrar WB, Goldstein LJ, Gradishar WJ, Hayes DF, Hudis CA, Jahanzeb M, Kiel K, Ljung BM, Marcom PK, Mayer IA, McCormick B, Nabell LM, Pierce LJ, Reed EC, Smith ML, Somlo G, Theriault RL, Topham NS, Ward JH, Winer EP, Wolff AC. NCCN Breast Cancer Clinical Practice Guidelines Panel (2009) Breast cancer. Clinical practice guidelines in oncology. *J Natl Compr Canc Netw* **7**: 122–192.

Deryugina EI, Bourdon MA, Jungwirth K, Smith JW, Strongin AY (2000) Functional activation of integrin alpha V beta 3 in tumor cells expressing membrane-type 1 matrix metalloproteinase. *Int J Cancer* **86**(1): 15–23.

Folmer F, Jaspars M, Solano G, Cristofanon S, Henry E, Tabudravu J, Black K, Green DH, Küpper FC, Aalbersberg W, Feussner K, Dicato M, Diederich M (2009) The inhibition of TNF-α induced NF-κB activation by marine natural products. *Biochem Pharmacol* **78**: 592–606.

Honn KV, Tang DG, Grossi I, Duniec ZM, Timar J, Renaud C, Leithauser M, Blair I, Johnson CR, Diglio CA, Kimler VA, Taylor JD, Marnett LJ (1994) Tumour cell-derived 12(S)-hydroxyeicosatetraenoic acid induces microvascular endothelial cell retraction. *Cancer Res* **54**: 565–574.

Honn KV, Grossi IM, Diglio CA, Wojtukiewicz M, Taylor JD (1989) Enhanced tumor cell adhesion to the subendothelial matrix resulting from 12(S)-HETE-induced endothelial cell retraction. *FASEB J* **3**(11): 2285–2293.

Jenkinson SR, Barraclough R, West CR, Rudland PS (2004) S100A4 regulates cell motility and invasion in an in vitro model for breast cancer metastasis. *Br J Cancer* **90**: 253–262.

Kerjaschki D, Bago-Horvath Z, Rudas M, Sexl V, Schneckenleithner C, Wolbank S, Bartel G, Krieger S, Kalt R, Hantusch B, Keller T, Nagy-Bojarszky K, Huttary N, Raab I, Lackner K, Krautgasser K, Schachner H, Kaserer K, Rezar S, Madlener S, Vonach C, Davidovits A, Nosaka H, Hämmerle M, Viola K, Dolznig H, Schreiber M, Nader A, Mikulits W, Gnant M, Hirakawa S, Detmar M, Alitalo K, Nijman S, Offner F, Maier TJ, Steinhilber D, Krupitza G (2011) Lipoxygenase mediates invasion of intrametastatic lymphatic vessels and propagates lymph node metastasis of human mammary carcinoma xenografts in mouse. *J Clin Invest* **121**(5): 2000–2012.

Madlener S, Saiko P, Vonach C, Viola K, Huttary N, Stark N, Popescu R, Gridling M, Vo NT, Herbacek I, Davidovits A, Giessrigl B, Venkateswarlu S, Geleff S, Jäger W, Grusch M, Kerjaschki D, Mikulits W, Golakoti T, Fritzer-Szekeres M, Szekeres T, Krupitza G (2010) Multifactorial anticancer effects of digalloyl-resveratrol encompass apoptosis, cell-cycle arrest, and inhibition of lymphendothelial gap formation *in vitro*. *Br J Cancer* **102**(9): 1361–1370.

Nishimura A, Akeda K, Matsubara T, Kusuzaki K, Matsumine A, Masuda K, Gemba T, Uchida A, Sudo A (2011) Transfection of NF-κB decoy oligodeoxynucleotide suppresses pulmonary metastasis by murine osteosarcoma. *Cancer Gene Ther* **18**(4): 250–259.

Orlowski RZ, Baldwin Jr AS (2002) NF-κB as a therapeutic target in cancer. *Trends Mol Med* **8**(8): 385–389.

Rice RL, Tang DG, Hddadi M, Honn KV, Taylor JD (1998) 12(S)-Hydroxyeicosatetraenoic acid increases microfilament content in B16a melanoma cells: a protein kinase-dependent process. *Int J Cancer* **77**: 271–278.

Schmidt-Hansen B, Ornås D, Grigorian M, Klingelhöfer J, Tulchinsky E, Lukanidin E, Ambartsumian N (2004) Extracellular S100A4 (mts1) stimulates invasive growth of mouse endothelial cells and modulates MMP-13 matrix metalloproteinase activity. *Oncogene* **23**: 5487–5495.

Schoppmann SF, Soleiman A, Kalt R, Okubo Y, Benisch C, Nagavarapu U, Herron GS, Geleff S (2004) Telomerase-immortalized lymphatic and blood endothelial cells are functionally stable and retain their lineage specificity. *Microcirculation* **11**: 261–269.

Spector AA, Gordon JA, Moore SA (1988) Hydroxyeicosatetraenoic acids (HETEs). *Prog Lipid Res* **27**: 271–323.

Srivastava RK, Kurzrock R, Shankar S (2010) MS-275 sensitizes TRAIL-resistant breast cancer cells, inhibits angiogenesis and metastasis, and reverses epithelial-mesenchymal transition *in vivo*. *Mol Cancer Ther* **9**(12): 3254–3266.

Takenaga K, Nakamura Y, Endo H, Sakiyama S (1994) Involvement of S100-related calcium-binding protein pEL98 (or mts1) in cell motility and tumor cell invasion. *Jpn J Cancer Res* **85**: 831–839.

Tang DG, Timar J, Grossi IM, Renaud C, Kimler VA, Diglio CA, Taylor JD, Honn KV (1993) The lipoxygenase metabolite, 12(S)-HETE, induces a protein kinase C-dependent cytoskeletal rearrangement and retraction of microvascular endothelial cells. *Exp Cell Res* **207**: 361–375.

Uchide K, Sakon M, Ariyoshi H, Nakamori S, Tokunaga M, Monden M (2007) Cancer cells cause vascular endothelial cell retraction via 12(S)-HETE secretion; the possible role of cancer cell derived microparticle. *Ann Surg Oncol* **14**: 862–868.

Vonach C, Viola K, Giessrigl B, Huttary N, Raab I, Kalt R, Krieger S, Vo TPN, Madlener S, Bauer S, Marian B, Hämmerle M, Kretschy N, Teichmann M, Hantusch B, Stary S, Unger C, Seelinger M, Eger A, Mader R, Jäger W, Schmidt W, Grusch M, Dolznig H, Mikulits W, Krupitza G (2011) NF-κB mediates the 12(S)-HETE-induced endothelial to mesenchymal transition of lymphendothelial cells during the intravasation of breast carcinoma cells. *Br J Cancer* **105**(2): 263–271.

Zeisberg M, Neilson EG (2009) Biomarkers for epithelial-mesenchymal transitions. *J Clin Invest* **119**(6): 1429–1437.